Journal of Power Sources 196 (2011) 5256–5263

Contents lists available at ScienceDirect

Journal of Power Sources

journal homepage: www.elsevier.com/locate/jpowsour

Development of group 4 and 5 metal oxide-based cathodes for polymer electrolyte fuel cell

Ken-ichiro Ota[1], Yoshiro Ohgi, Kyung-Don Nam, Koichi Matsuzawa, Shigenori Mitsushima, Akimitsu Ishihara*

Chemical Energy Laboratory, Yokohama National University, 79-5 Tokiwadai, Hodogaya-ku, Yokohama, Kanagawa 240-8501, Japan

ARTICLE INFO

Article history:
Received 17 June 2010
Received in revised form 5 September 2010
Accepted 8 September 2010
Available online 16 September 2010

Keywords:
Oxygen reduction reaction
Non-platinum cathode
Polymer electrolyte fuel cell
Non-noble metal oxide

ABSTRACT

Partially oxidized zirconium, niobium, and tantalum carbonitrides were prepared to discuss a characteristic common to all. The onset potential for the ORR of partially oxidized carbonitrides reached above ca. 0.85 V. The XRD and XPS analyses suggested that both the crystalline structure and the chemical bonding state of the surface of the partially oxidized carbonitrides were very similar to those of the oxides. However, the partially oxidized carbonitrides had lower ionization potential than the oxides. The lower ionization potential indicated that the partially oxidized carbonitrides had some defects on the surface. From these results, the structure of oxides and the highest oxidation state of surface metal with some oxygen defects were essential to have high ORR activity for group 4 and 5 oxide-based compounds. Such oxygen defects might be responsible for the oxygen reduction capability by creating electronically favorable oxygen adsorption sites.

1. Introduction

Polymer electrolyte fuel cells (PEFCs) are expected to be as power sources for residential cogeneration systems and transportation applications due to their high theoretical energy efficiency and less emission of pollutants. However, PEFCs have some serious problems to be solved for their commercialization. In particular, a large overpotential of the oxygen reduction reaction (ORR) must be reduced in order to obtain higher energy efficiency. A large amount of platinum is generally used as a cathode catalyst in the present PEFCs to decrease the overpotential of the ORR. However, Pt is expensive and its resources are limited so that the Pt usage will be limited in the future commercialization of PEFCs. Many researches have been tried to reduce the use of Pt catalyst such as a greater dispersion of Pt particles and/or alloying with transition metals [1,2]. However, because the dissolution and deposition of highly dispersion Pt particles proceeds during long-term operation [3], the drastic reduction of Pt usage would be difficult. Therefore, the development of a new non-platinum catalyst is strongly required.

Many studies have been performed to develop non-platinum cathode catalysts for low-temperature fuel cells. Organometallic complexes and chalcogenides were famous as candidates for an alternative Pt catalyst. Jasinski firstly introduced a cobalt phthalocyanine as an electrocatalyst for the ORR in 35% KOH in 1964 [4]. Jahnke and Schönborn applied transition metal phthalocyanines to the non-Pt cathode catalysts in 4.5 N H_2SO_4 in 1969 [5]. Many organometallic complexes have been widely investigated since then [6,7]. Bashyam and Zelenay showed that the cobalt-polypyrrole composite catalyst enabled power densities of about 0.15 Wcm^{-2} in H_2–O_2 fuel cells and displayed no signs of performance degradation for more than 100 h [8]. In recent years, Lefevre et al. reported that iron-based catalysts exhibited the similar performance of platinum supported carbon although the catalyst loading was much greater than that of Pt [9]. However, these catalysts have poor stability in an acid media such as H_2SO_4 and polymer electrolytes.

Alonso-Vante and Tributsch found that $Mo_{4.2}Ru_{1.8}Se_8$ had a catalytic activity for the ORR in acidic media in 1986 [10]. Alonso-Vante and co-workers reported that Ru acted as active site and Ru metal was protected against oxidation to Ru oxides by the chalcogens additives [11]. RuSe, RuTe, MoReSe, MoRhS, MoOsS, MoSe, ReRuS, IrRuS, (RuMo)SeO, WRuSe, RhS, RhSe, RuCrSe, RuFeSe, and CoSe were investigated besides MoRuSe [12]. Because these chalcogenides were inactive for methanol, the development for cathodes as direct methanol fuel cells was examined. However, Ru and Rh are precious metals and their resources are very limited. The researches on these non-platinum catalysts were summarized by some reviews [13,14]. These catalysts have neither a sufficient electrocatalytic activity for the ORR nor a long-term stability.

We believe that a high stability is an essential requirement for a cathode of PEFCs because the cathode catalysts are exposed

* Corresponding author. Tel.: +81 45 339 4022; fax: +81 45 339 4024.
E-mail address: a-ishi@ynu.ac.jp (A. Ishihara).
[1] ISE member.

0378-7753/$ – see front matter © 2010 Elsevier B.V. All rights reserved.
doi:10.1016/j.jpowsour.2010.09.021

to an acidic and oxidative atmosphere, that is, a strong corrosive environment. We have reported that tungsten carbide with tantalum addition [15], tantalum oxynitride [16–19], zirconium oxide [20–22], titanium oxide [23], zirconium oxynitride [24,25], chromium carbonitride [26] and tantalum carbonitride [27] were stable in an acid solution and had a definite catalytic activity for the ORR. In recent years, we found that the partially oxidized group 4 and 5 metal carbonitrides powder had a definite catalytic activity for the ORR [28–31]. However, these researches are discussed separately. In the present paper, we prepared some catalysts such as partially oxidized zirconium, niobium, and tantalum carbonitrides and a characteristic common to these compounds was discussed. We control a degree of oxidation of the carbonitride powders by control of condition of partial oxidation. In case of tantalum, the degree of oxidation of carbonitride powders was varied with different heat treatment time to obtain partially oxidized carbonitride powders with different oxidation states [28]. In the present paper, we treated considerably oxidized carbonitride powders as representatives of partially oxidized specimens.

2. Experimental

2.1. Sample preparation

Zirconium, niobium, and tantalum carbonitride powders were used as starting materials. A mixture of ZrO_2 powder and carbon black was heated at 1800 °C under nitrogen atmosphere to synthesize zirconium carbonitride. Niobium carbonitride powder was synthesized by using a mixture of Nb powder (<45 μm, 99.9%, High Purity Chemicals, Japan) and carbon black. The mixture of Nb and carbon black powder was heat-treated in an alumina tube furnace in N_2 atmosphere at 1500 °C for 10 h. Ta_2O_5 powder and carbon black were uniformly mixed, and the mixture was heat-treated at 1600 °C under flowing N_2 to make tantalum carbonitride. The carbon content of the these carbonitrides was determined with an infrared absorption method after combustion by high-frequency induction using a high frequency infrared carbon–sulfur analyzer instrument (CS-600 series, LECO Japan Co., Japan). The nitrogen and oxygen contents of the carbonitrides were determined using inert-gas fusion thermal conductivity method and inert gas fusion-infrared absorption method (TCH600 series, LECO Japan Co., Japan), respectively. The overall chemical compositions of the zirconium carbonitride, niobium carbonitride, and tantalum carbonitride were determined to be $ZrC_{0.5}N_{0.5}$, $NbC_{0.5}N_{0.5}$, and $TaC_{0.58}N_{0.42}$, respectively.

The $ZrC_{0.5}N_{0.5}$, $NbC_{0.5}N_{0.5}$, and $TaC_{0.58}N_{0.42}$ powders were heat-treated using a vacuum purge electric furnace at 900 °C for several hours under a flow rate of 100 $cm^3\ min^{-1}$ of the 2%-H_2/N_2 gas containing 0.5% oxygen to obtain partially oxidized specimens. In this paper, partially oxidized $ZrC_{0.5}N_{0.5}$, $NbC_{0.5}N_{0.5}$, and $TaC_{0.58}N_{0.42}$ were expressed as Zr–CNO, Nb–CNO, and Ta–CNO, respectively.

2.2. Electrochemical measurements

In order to evaluate the catalytic activity for the ORR, the working electrode was prepared as follows. The carbonitrides with and without heat treatment powders and oxides were mixed with Ketjen Black (5 wt.%) because mixture with the carbon black as a current collector was found to be useful to increase the ORR current [28]. The mixture was suspended in a mixture of 1-propanol and distilled water. The suspension was evenly dropped onto the glassy carbon rod (5.2 mmφ). The catalyst loading was about 2 mg on the glassy carbon rod. Dilute Nafion® solution (0.5 wt.%), then, was dropped onto the surface. The coated glassy carbon rod was dried in inert atmosphere at 120 °C for 1 h with a drying oven to prepare a working electrode. Electrochemical measurements were carried out in 0.1 mol dm^{-3} H_2SO_4 at 30 °C in N_2 and O_2 using a three-electrode cell. A reversible hydrogen electrode (RHE) and the carbon plate were used as a reference and counter electrode, respectively. In order to stabilize the electrode, cyclic voltammetry was carried out from 0.05 to 1.2 V vs. RHE in N_2 at a scan rate of 50 mV s^{-1}. When cyclic voltammetry reached a steady state, slow scan voltammetry (SSV) was measured from 0.2 to 1.2 V vs. RHE in N_2 and O_2 at a scan rate of 5 mV s^{-1} to obtain the potential–current curves for the ORR. The difference between the current under O_2 (i_{O_2}) and that under N_2 (i_{N_2}) was corresponded to the oxygen reduction current (i_{ORR}), that is, $i_{ORR} = i_{O_2} - i_{N_2}$. The current density was based on the geometric area of the working electrode. The onset potential for the ORR, E_{ORR}, was defined as the electrode potential at the $i_{ORR} = -0.2$ μA cm^{-2}. The onset potential was utilized to evaluate the catalytic activity for the ORR in the present study.

2.3. Characterization

The crystalline structure of the specimens was characterized using an X-ray diffractometer (XRD; XRD-6000, Shimadzu, Japan) with Cu Kα in the range from 15 to 85°. An X-ray photoelectron spectroscopy (XPS; AXIS-NOVA, Kratos, US) was performed to investigate the chemical bonding state of the surface of the specimens at the accelerating voltage of 10 kV. The peak of the C–C bond attributed to free carbon at 284.6 eV in C 1s spectrum was used to compensate for surface charging in XPS. An ionization potential of specimens was measured using a photoelectron spectrometer surface analyzer (Model AC-3, Riken Keiki) [32].

3. Results and discussion

3.1. Crystalline structure

Fig. 1 illustrates the XRD patterns of (a) $ZrC_{0.5}N_{0.5}$, Zr–CNO, and commercial ZrO_2 (Wako Pure Chemicals Co., Japan) and (b) $NbC_{0.5}N_{0.5}$, Nb–CNO, and Nb_2O_5, and (c) $TaC_{0.58}N_{0.42}$, Ta–CNO, and commercial Ta_2O_5 (High Purity Chemicals, Japan). Nb_2O_5 was prepared by complete oxidation of $NbC_{0.5}N_{0.5}$ with heat treatment at 900 °C under atmospheric condition.

In all cases, both these carbides and nitrides have a same crystalline structure (Rock-Salt type) and form a complete solid solution. The peak pattern does not change from carbide to nitride, and an each peak shifts to higher angle with the increase of nitrogen content, which is known as the Vegard's law [33]. In the present paper, the compounds with XRD peaks which existed between ZrC (JCPDS: 35-0784) and ZrN (JCPDS: 35-0753), NbC (JCPDS: 38–1364) and NbN (JCPDS: 38–1155), and TaC (JCPDS: 35-0801) and TaN (JCPDS: 32-1283) were expressed as ZrC_xN_y, NbC_xN_y, and TaC_xN_y, respectively. No peaks due to oxides were observed in these carbonitrides in all cases.

The Zr–CNO, Nb–CNO, and Ta–CNO, which were considerably oxidized, had only oxides peaks, as shown in Fig. 1. However, although the XRD patterns indicated that the Zr–CNO, Nb–CNO, and Ta–CNO were identified as ZrO_2 (JCPDS: 37-1484), Nb_2O_5 (JCPDS: 37-1468), and Ta_2O_5 (JCPDS: 25-0922), respectively, the color of the partially oxidized specimens was not white but black. These XRD patterns show that these partially oxidized carbonitride powders had similar crystalline structure to these oxides.

3.2. Catalytic activity for the oxygen reduction reaction

In electrochemical measurements, after the cyclic voltammogram reached steady state, slow scan voltammetry (scan rate: 5 mV s^{-1}, 1.2–0.2 V) was performed under nitrogen or oxygen atmosphere in 0.1 mol dm^{-3} H_2SO_4 at 30 °C. Potential–current

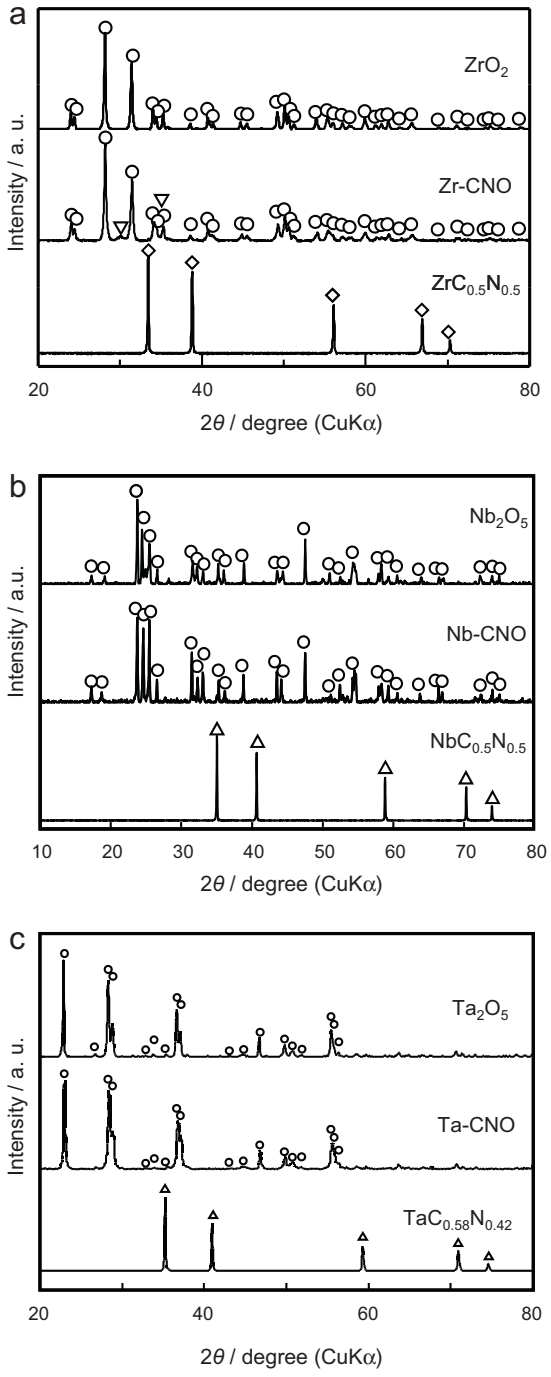

Fig. 1. XRD patterns of (a) $ZrC_{0.5}N_{0.5}$, Zr–CNO, and commercial ZrO_2 (Wako Pure Chemicals Co., Japan) and (b) $NbC_{0.5}N_{0.5}$, Nb–CNO, and Nb_2O_5, and (c) $TaC_{0.58}N_{0.42}$, Ta–CNO, and commercial Ta_2O_5 (High Purity Chemicals, Japan). (a) ♢: ZrC_xN_y, ▽: cubic-ZrO_2 (JCPDS: 49-1642), ○: monoclinic-ZrO_2 (JCPDS: 37-1484), (b) △: NbC_xN_y, ○: Nb_2O_5 (JCPDS: 37-1468), (c) △: TaC_xN_y, ○: Ta_2O_5 (JCPDS: 25-0922).

curves observed in the slow scan voltammetry immediately reached steady state. The potential–current curve at 3rd cycle with cathodic scan was chosen to obtain the ORR current. Fig. 2 shows the potential–ORR current curves of the (a) Zr-based compounds, (b) Nb-based compounds, (c) Ta-based compounds in 0.1 mol dm^{-3} H_2SO_4 at 30 °C with a scan rate of 5 mV s^{-1}. In all cases, the ORR current of the carbonitrides and the oxides was observed below 0.6 V, indicating that the carbonitrides and the oxides had poor catalytic activity toward the ORR. On the other hand, the ORR current of the partially oxidized carbonitrides was clearly observed at

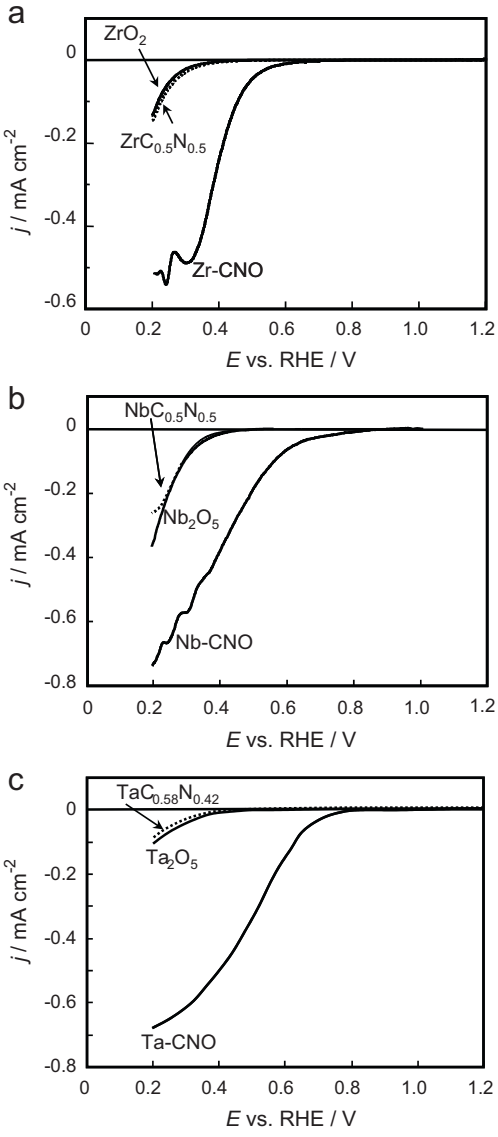

Fig. 2. Potential–i_{ORR} curves of (a) Zr-based compounds, (b) Nb-based compounds, (c) Ta-based compounds in 0.1 mol dm^{-3} H_2SO_4 at 30 °C with a scan rate of 5 mV s^{-1}.

higher potential. Therefore, it was found that the partial oxidation of group 4 and 5 metal carbonitrides was greatly useful to enhance the catalytic activity for the ORR.

Fig. 3 shows the onset potential for the ORR in 0.1 mol dm^{-3} H_2SO_4 at 30 °C. Although the carbonitrides have some electrical conductivity and some stability in an acid solution, the carbonitrides have poor ORR activity because these onset potentials are very low. In addition, the oxides also have poor ORR activity as expected. On the other hand, these partially oxidized carbonitrides have higher onset potential around 0.85 V or above. The onset potential increased about 0.3–0.35 V with the partial oxidation.

In the case of tantalum, a partial oxidation, that is, the substitution for O atoms, brings an increase in ionic components among the chemical bonding, because the energy difference between the Ta 5d and O 2p orbitals is higher than that between Ta 5d and C or N 2p. The partial oxidation method might produce the oxygen defects, which formed the release point of C and/or N, and/or remaining C or N on the surface. In the case of zirconium and niobium, it seems that a similar phenomenon has occurred.

The onset potential of Pt/C (Pt loading: 46.3 wt.%; Tanaka Kikinzoku Kogyo) was 1.05 V. The catalytic activity of the partially

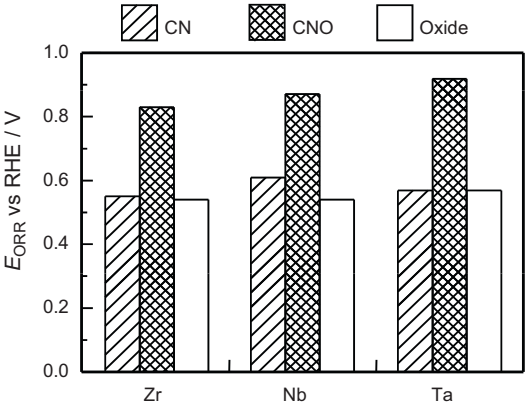

Fig. 3. Onset potential for ORR in 0.1 mol dm^{-3} H_2SO_4 at 30 °C with a scan rate of 5 mV s^{-1}.

oxidized carbonitrides was much lower than that of the Pt/C at present. However, preparation of ultra-fine particle and increase in density of active sites on the surface would enhance the ORR activity. Therefore, the partially oxidized carbonitrides might be possible candidate as alternative Pt cathode for PEFC.

3.3. Characterization of the specimens

The chemical bonding state of the surface was analyzed using an X-ray photoelectron spectroscopy (XPS). Fig. 4 shows the XPS of (a) Zr 3d, (b) O 1s, (c) N 1s, and (d) C 1s of the $ZrC_{0.5}N_{0.5}$, the Zr–CNO, and the ZrO_2. The value of binding energy for Zr $3d_{5/2}$ reported in the literature for Zr^{4+} in pure zirconia was 182.26 eV [34]. However, the measured value of binding energy for Zr $3d_{5/2}$ of ZrO_2 in the present study, 181.8 eV, was slightly smaller than that of the literature. We used the 181.8 eV as the binding energy of Zr $3d_{5/2}$ of ZrO_2 in the present study. In the case of $ZrC_{0.5}N_{0.5}$, two peaks were complicated in Zr 3d spectra. One shifted lower than ZrO_2, and another existed higher. The binding energy of Zr $3d_{5/2}$ of ZrN was ca. 179.8 eV [35]. ZrC probably had similar binding energy of Zr $3d_{5/2}$. Therefore, the lower Zr $3d_{5/2}$ peak, ca. 179.8 eV, was attributed to carbonitride. The peaks attributed to ZrN (N 1s ZrN: 397.3 eV [36]) was observed in N 1s spectra of $ZrC_{0.5}N_{0.5}$. In addition, in C 1s spectra there were small peak at around 282 eV which was responsible for ZrC (C 1s ZrC: 281.5 eV [37]) as well as free carbon (C 1s: 285 eV). These results also supported that zirconium carbonitride existed near the surface of the $ZrC_{0.5}N_{0.5}$. Another peak, Zr $3d_{5/2}$ of ca. 182.2 eV, was probably responsible for the hydroxide. The O 1s spectra of the $ZrC_{0.5}N_{0.5}$ had a large shoulder around 531.6 eV. The peak due to hydroxide positioned at 531.6 eV [38]. The Zr 3d and O 1s spectra of the $ZrC_{0.5}N_{0.5}$ suggested that some of oxide transformed to hydroxide on the surface. These results indicated that the surface of the $ZrC_{0.5}N_{0.5}$ powder was slightly oxidized in air, and the oxides partially transformed hydroxides on the surface. In O 1s spectra of the Zr–CNO, the shoulder attributed to hydroxide at 531.6 eV decreased with the partial oxidation. In addition, the peak due to carbonitride in the Zr 3d spectrum of the Zr–CNO powders disappeared and no nitride and carbide peaks in N 1s and C 1s were observed in the Zr–CNO. These results suggested that the surface of the Zr–CNO was oxidized due to the partial oxidation and the hydroxide on the surface transformed to oxide by the heat treatment. Little difference was observed in the XPS spectra between the Zr–CNO and the ZrO_2.

Fig. 5 shows the XPS spectra of the $NbC_{0.5}N_{0.5}$, the Nb–CNO, and the Nb_2O_5 in (a) Nb 3d, (b) O 1s, (c) N 1s, and (d) C 1s regions. As shown in Fig. 5(c) and (d), the $NbC_{0.5}N_{0.5}$ had peaks identified as NbC (282.8 eV) [39] and NbN (397.2 eV) [40]. The binding

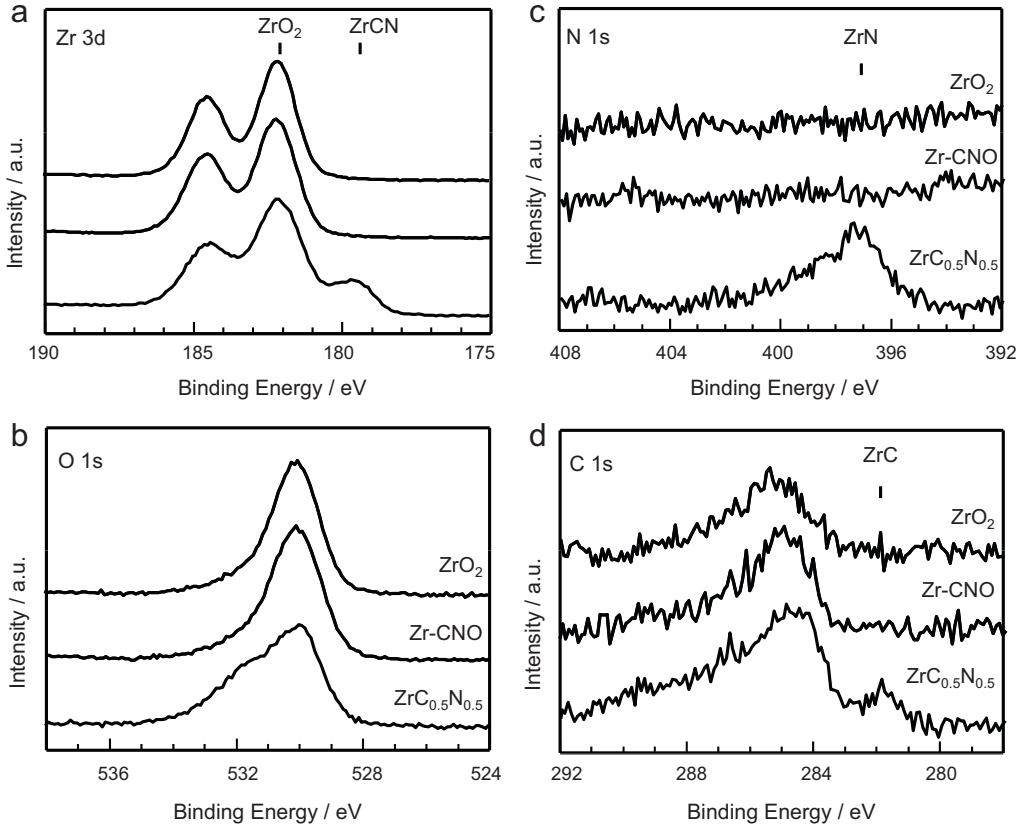

Fig. 4. XPS of (a) Zr 3d, (b) O 1s, (c) N 1s, and (d) C 1s.

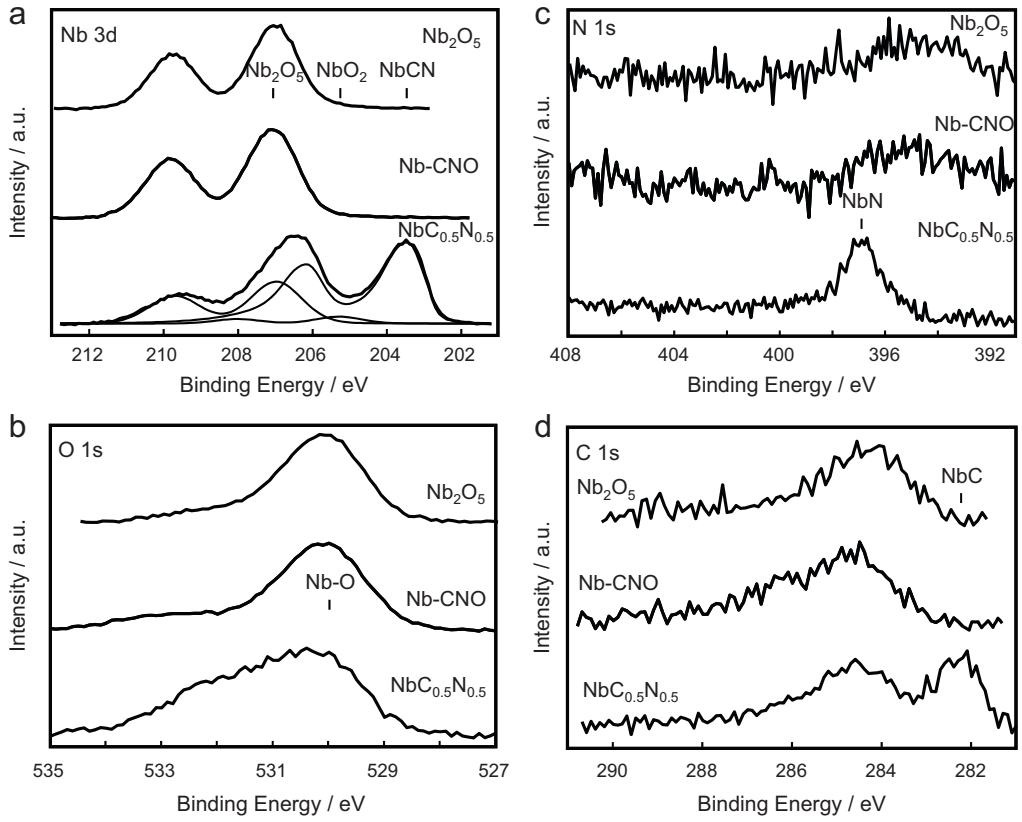

Fig. 5. XPS of (a) Nb 3d, (b) O 1s, (c) N 1s, and (d) C 1s.

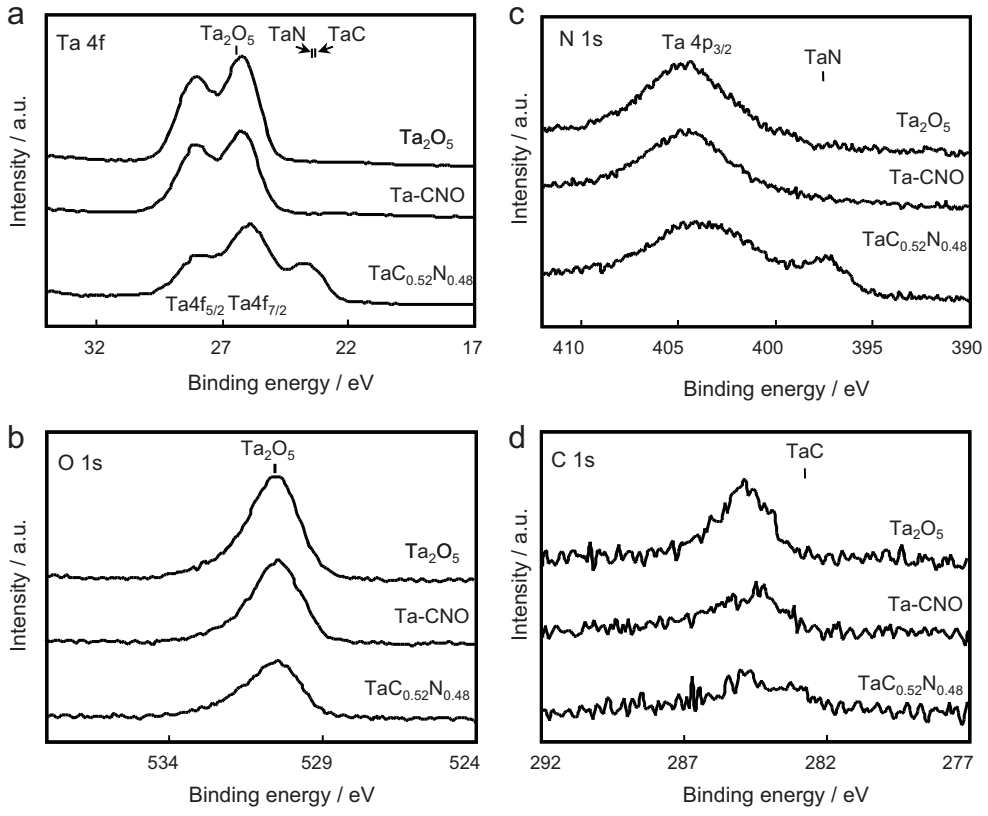

Fig. 6. XPS of (a) Ta 4f, (b) O 1s, (c) N 1s, and (d) C 1s.

energies of Nb $3d_{5/2}$ peaks corresponding to NbC and NbN were 203.7 [41] and 203.8 eV [42], respectively. Niobium forms oxides in various oxidation states, i.e., NbO_2 (Nb^{4+}) at a binding energy of 205.5–206.0 eV, and Nb_2O_5 (Nb^{5+}) at 207.0–207.6 eV [41,43]. Three peaks were superimposed in the Nb $3d_{5/2}$ spectrum of the $NbC_{0.5}N_{0.5}$. The first peak was positioned near the peak of NbC or NbN, and the second peak located at the peak of NbO_2 was very small. The third peak was identified as Nb_2O_5. This result indicated that the surface of the $NbC_{0.5}N_{0.5}$ was mainly composed of NbC_xN_y and Nb_2O_5. Although the XRD pattern of the $NbC_{0.5}N_{0.5}$ had only NbC_xN_y peaks, the surface of the $NbC_{0.5}N_{0.5}$ powder was slightly oxidized in air. In O 1s spectra, the shoulder attributed to hydroxide decreased with the partial oxidation in the same as Zr. The Nb 3d peak of the Nb–CNO powders shifted to higher energy and no nitride and carbide peaks in N 1s and C 1s were observed in the Nb–CNO. Therefore, the surface of the Nb–CNO was considerably oxidized similar to Nb_2O_5.

Fig. 6(a)–(d) shows the XPS of Ta 4f, O 1s, C 1s, and N 1s. Peak positions of Ta_2O_5 (26.5 eV), TaN (23.5 eV), and TaC (23.3 eV) in Fig. 6(a) correspond to those of Ta $4f_{7/2}$ [44–46]. Two peaks were superimposed in the Ta $4f_{7/2}$ spectrum of the $TaC_{0.52}N_{0.48}$. One peak was positioned near the peak of TaC or TaN, and another was located at the peak of Ta_2O_5. This result indicated that the surface of the TaC_xN_y was composed of TaC_xN_y and Ta_2O_5. In addition, the peaks attributed to TaN (397.6 eV) [47] and to TaC (282.6 eV) [47] were observed in the N 1s and C 1s spectra of the $TaC_{0.52}N_{0.48}$, respectively. Although the XRD pattern of the $TaC_{0.52}N_{0.48}$ had only TaC_xN_y peaks, the surface of the $TaC_{0.52}N_{0.48}$ powder was partially oxidized in air.

No peaks attributed to the carbonitride were observed on the Ta–CNO as shown in Fig. 6(a), (c), and (d). From the peaks of Ta $4f_{7/2}$ and O 1s, only Ta_2O_5 was detected on the surface of the Ta–CNO. Little difference was observed between the Ta–CNO and the Ta_2O_5 in the XPS. The results of the XPS suggested that the highest oxidation state of metals was probably essential to have high ORR activity.

The ionization potential of the specimens was measured using a photoelectron spectrometer surface analyzer to reveal the difference of the surface electronic state between the partially oxidized carbonitrides and the oxides. Fig. 7 shows the relationship between the square root of the photoelectric quantum yield $Y^{1/2}$ and the photon energy, that is, the photoelectron spectra of the (a) Zr-based compounds, (b) Nb-based compounds, and (c) Ta-based compounds. The beam power was 200 nW. Because the carbonitrides were electrical conductors, the photoelectrons were emitted at low photon energy in all carbonitrides. The photoelectrons were difficult to emit with the progress of the oxidation. The square root of the photoelectric quantum yield increased almost linearly with increasing the photon energy on each specimen. The slope of the straight line reflected the tendency of the photoelectron emission of the specimens, that is, the density of state of the electrons near the Fermi level. The slopes of the oxides were apparently lower than that of carbonitrides and partially oxidized carbonitrides, because oxides are insulators. It is remarkable that the partially oxidized specimens had higher slope than the oxides, indicating that the partially oxidized specimens had larger density of state of electrons than the oxides near the Fermi level. The intersection between the straight line and the background line in the photoelectron spectra provided a threshold energy. The threshold energy corresponded to a photoelectric ionization potential, which accorded with the work function in case of metals. As shown in Fig. 7, the ionization potentials of the $ZrC_{0.5}N_{0.5}$, the $NbC_{0.5}N_{0.5}$, and the $TaC_{0.52}N_{0.48}$ were 5.08, 4.81, and 4.75 eV, respectively. The work functions of metal Zr, Nb, and Ta were 4.05, 4.3, and 4.25 eV, respectively [48]. The ionization potential of the $ZrC_{0.5}N_{0.5}$, the $NbC_{0.5}N_{0.5}$, and the $TaC_{0.52}N_{0.48}$ were ca. 1.0, 0.6, and 0.5 eV larger than those of these metals because of the carbonitridation. In the case of the oxides, the

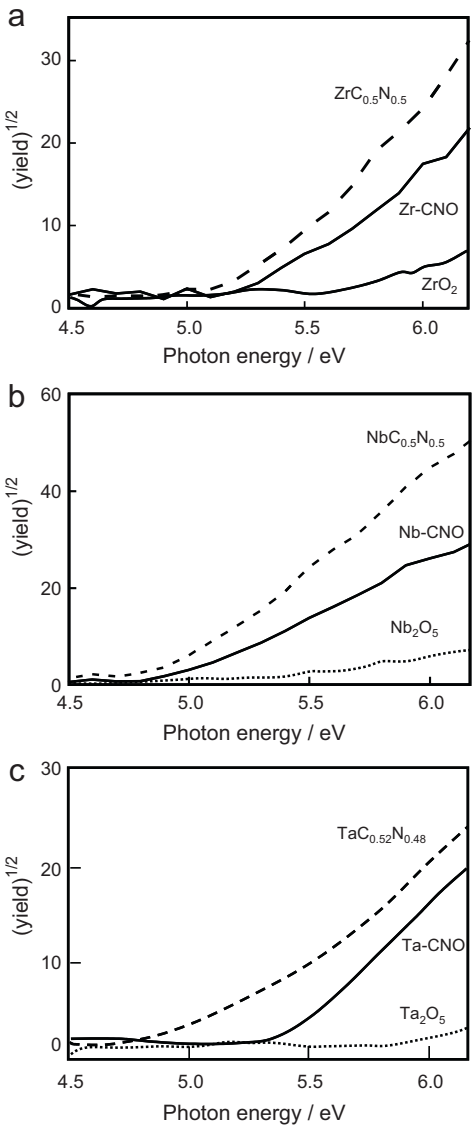

Fig. 7. Relationship between square root of photoelectric quantum yield $Y^{1/2}$ and the photon energy of (a) Zr-based compounds, (b) Nb-based compounds, and (c) Ta-based compounds. Beam power: 200 nW.

ionization potentials of the ZrO_2, the Nb_2O_5, and the Ta_2O_5 were determined to be 5.56, 5.53, and 5.8 eV, respectively. The highest energy level of electrons in the valence band of bulk ZrO_2, Nb_2O_5, and Ta_2O_5 is reported to be ca. −7.5, −7.6, and −7.8 eV [49], that is, the ionization potentials of ZrO_2, Nb_2O_5, and Ta_2O_5 are predicted to be ca. 7.5, 7.6, 7.8 eV, respectively. However, the ionization potential of the ZrO_2, the Nb_2O_5, and the Ta_2O_5 obtained was no less than ca. 2.0 eV lower than that predicted from literature. The surface level of the oxides probably caused the lower ionization potential.

As shown in Fig. 7, the ionization potentials of the Zr–CNO, the Nb–CNO, and the Ta–CNO were 5.12, 4.84 and 5.25 eV, respectively. The XRD and XPS analysis suggested that the physical properties such as the crystalline structure and the chemical bonding state of the surface of the partially oxidized carbonitrides were similar to those of the oxides. However, the ionization potential and the density of state of the electrons near the Fermi level in these specimens were obviously different. The ionization potential of the partially oxidized carbonitrides obtained in the present study was much lower than that of the oxides.

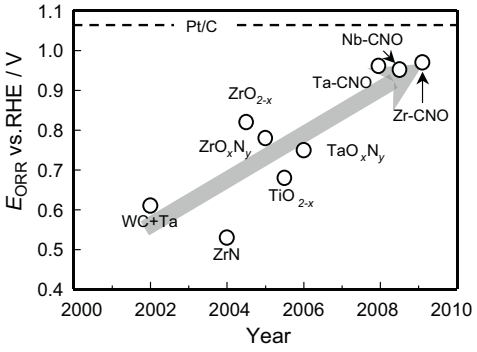

Fig. 8. Onset potential for oxygen reduction reaction of non-precious metal oxide-based cathodes developed at Yokohama National University (0.1 mol dm^{-3} H_2SO_4, 30 °C).

Henrich et al. found that the work function of the oxides decreased with increasing the density of defects [50]. Therefore, the low ionization potential suggested that the partially oxidized carbonitrides had some surface defects. Lattice defects and impurities introduce localized electron levels in the band gap of metal oxides. Vacancies of oxide ion give donor levels close to the edge level of the conduction band [51]. Therefore, we think that the partially oxidized carbonitrides probably had some vacancies of oxide ion [52]. The adsorption of oxygen molecules on the surface was required as the first step to proceed the ORR. Many researchers found that the surface defects sites were required to adsorb the oxygen molecules on the surface of the oxides [53–57]. Therefore, the increase in the surface defects on the partially oxidized carbonitrides yielded the increase in the adsorption sites of oxygen molecules. In addition, the interaction of oxygen with the catalyst surface is essentially important because both the adsorption of oxygen and the desorption of water on the surface is necessary to continue the fluent progress of the ORR. When the interaction of oxygen with the catalyst surface is strong, the desorption of water is restrained. On the other hand, when the interaction of oxygen with the catalyst surface is weak, few adsorption of oxygen molecules proceeds. Therefore, there is suitable strength of the interaction between the oxygen and the catalyst surface. Metal Zr, Nb, and Ta strongly adsorbed oxygen because of the large calculated adsorption enthalpies of oxygen (Zr: 824, Nb: 832, and Ta: 937 kJ mol^{-1}) [58]. In case of Pt, the adsorption energy of oxygen of Pt was 280 kJ mol^{-1} [58]. Therefore, calculated adsorption enthalpies of oxygen of Zr, Nb, and Ta were much larger than that of Pt. As the oxidization of metal Zr, Nb, and Ta proceeded, the interaction of oxygen with these metals of the catalyst surface became weak because the oxide ions attracted the electrons of the highest occupied molecule orbital of metal to be metal charged positively. When the interaction between the surface metals and oxygen become suitable for the ORR, the ORR proceeded fluently. From the experimental results, the structure of oxides and the highest oxidation state of surface metal with some oxygen defects were essential to have high ORR activity for group 4 and 5 oxide-based compounds. Such oxygen defects might be responsible for the oxygen reduction capability by creating electronically favorable oxygen adsorption sites.

Fig. 8 shows the summary of the onset potentials of new catalysts prepared by Yokohama group without platinum group metals for the ORR. Among these materials, partially oxidized carbonitrides had higher catalytic activity for the ORR. The highest onset potentials of the Zr–CNO, the Nb–CNO, and the Ta–CNO, which were prepared under optimized conditions, were 0.97, 0.92, and 0.96 V, respectively. Although there is some difference in the ORR activity from a Pt/C catalyst, these materials have a great potential for PEFC cathode.

4. Conclusions

We prepared some catalysts such as partially oxidized zirconium, niobium, and tantalum carbonitrides and discussed a characteristic common to all. The catalytic activity for the ORR increased with partial oxidation. The XRD patterns of the partially oxidized carbonitrides were similar to those of the oxides. In addition, the XPS revealed that the surface chemical bonding state of the partially oxidized carbonitrides were similar to those of the oxides. However, the partially oxidized carbonitrides had lower ionization potential than the oxides. The lower ionization potential indicated that the partially oxidized carbonitrides had some defects on the surface. From these results, the structure of oxides and the highest oxidation state of surface metal with some oxygen defects were essential to have high ORR activity for group 4 and 5 oxide-based compounds. Such oxygen defects might be responsible for the oxygen reduction capability by creating electronically favorable oxygen adsorption sites.

The oxygen defects might be responsible for the oxygen reduction capability by creating electronically favorable oxygen adsorption sites.

Acknowledgements

The authors wish to thank A.L.M.T. Corp. for supply of the $ZrC_{0.5}N_{0.5}$ and $TaC_{0.52}N_{0.48}$, and Riken Keiki Co., Ltd. for measurement of the ionization potential. This work was performed under the "Non-precious metal oxide-based cathode for PEFC Project" supported by the New Energy and Industrial Technology Development Organization (NEDO).

References

[1] T. Toda, H. Igarashi, H. Uchida, M. Watanabe, J. Electrochem. Soc. 146 (1999) 3750.
[2] S. Mukerjee, S. Srinirasan, M.P. Soriaga, J. McBreen, J. Phys. Chem. 99 (1995) 4577.
[3] K. Yasuda, A. Taniguchi, T. Akita, T. Ioroi, Z. Siroma, J. Electrochem. Soc. 153 (2006) A1599.
[4] R. Jasinski, Nature 201 (1964) 1212.
[5] H. Jahnke, M. Schönborn, Comptes Rendus, Troisièmes Journées Internationales d'Etude des Piles à Combustible, vol. 60, Presses Académiques Européennes, Bruxelles, 1969.
[6] C.W.B. Bezerra, L. Zhang, K. Lee, H. Liu, A.L.B. Marques, E.P. Marques, H. Wang, J. Zhang, Electrochim. Acta 53 (2008) 4937.
[7] J.H. Zagal, in: W. Vielstich, A. Lamm, H.A. Gasteiger (Eds.), Handbook of Fuel Cells—Fundamentals Technology and Applications, vol. 2, John Wiley & Sons Ltd., West Sussex, 2003, pp. 545–554.
[8] R. Bashyam, P. Zelenay, Nature 443 (2006) 63.
[9] M. Lefevre, E. Proietti, F. Jaouen, J.P. Dodelet, Science 324 (2009) 71.
[10] N. Alonso-Vante, H. Tributsch, Nature 323 (1986) 431.
[11] A. Lewera, J. Inukai, W.P. Zhou, D. Cao, H.T. Duong, N. Alonso-Vante, Electrochim. Acta 52 (2007) 5759.
[12] N. Alonso-Vante, in: W. Vielstich, A. Lamm, H.A. Gasteiger (Eds.), Handbook of Fuel Cells—Fundamentals, Technology and Applications, vol. 2, John Wiley & Sons Ltd, West Sussex, 2003, pp. 534–543.
[13] Z. Shi, J. Zhang, Z.-S. Liu, H. Wang, D.P. Wilkinson, Electrochim. Acta 51 (2006) 1905.
[14] B. Wang, J. Power Sources 152 (2005) 1.
[15] K. Lee, A. Ishihara, S. Mitsushima, N. Kamiya, K. Ota, Electrochim. Acta 49 (2004) 3479.
[16] A. Ishihara, K. Lee, S. Doi, S. Mitsushima, N. Kamiya, M. Hara, K. Domen, K. Fukuda, K. Ota, Electrochem. Solid State Lett. 8 (2005) A201.
[17] Y. Shibata, A. Ishihara, S. Mitsushima, N. Kamiya, K. Ota, Electrochem. Solid State Lett. 10 (2007) B43.
[18] A. Ishihara, S. Doi, S. Mitsushima, K. Ota, Electrochim. Acta 53 (2008) 5442.
[19] Y. Ohgi, A. Ishihara, Y. Shibata, S. Mitsushima, K. Ota, Chem. Lett. 37 (2008) 608.
[20] Y. Liu, A. Ishihara, S. Mitsushima, N. Kamiya, K. Ota, Electrochem. Solid State Lett. 8 (2005) A400.
[21] Y. Liu, A. Ishihara, S. Mitsushima, N. Kamiya, K. Ota, J. Electrochem. Soc. 154 (2007) B664.
[22] Y. Liu, A. Ishihara, S. Mitsushima, N. Kamiya, K. Ota, Electrochim Acta, 55 (2010) 1239.
[23] J.-H. Kim, A. Ishihara, S. Mitsushima, N. Kamiya, K. Ota, Electrochim. Acta 52 (2007) 2492.

[24] S. Doi, A. Ishihara, S. Mitsushima, N. Kamiya, K. Ota, J. Electrochem. Soc. 154 (2007) B362.
[25] Y. Maekawa, A. Ishihara, S. Mitsushima, K. Ota, Electrochem. Solid State Lett. 11 (2008) B109.
[26] J.-H. Kim, A. Ishihara, S. Mitsushima, N. Kamiya, K. Ota, Chem. Lett. 36 (2007) 514.
[27] J.-H. Kim, A. Ishihara, S. Mitsushima, N. Kamiya, K. Ota, Electrochemistry 75 (2007) 166.
[28] A. Ishihara, Y. Shibata, S. Mitsushima, K. Ota, J. Electrochem. Soc. 155 (2008) B400.
[29] A. Ishihara, M. Tamura, K. Matsuzawa, S. Mitsushima, K. Ota, Electrochim. Acta (2009), doi:10.1016/j.electacta.2009.10.063.
[30] K.-D. Nam, A. Ishihara, K. Matsuzawa, S. Mitsushima, K. Ota, Electrochem. Solid State Lett. 12 (2009) B158.
[31] Y. Ohgi, A. Ishihara, K. Matsuzawa, S. Mitsushima, K. Ota, J. Electrochem. Soc. 157 (2010) B885.
[32] H. Kirihata, M. Uda, Rev. Sci. Instrum. 52 (1981) 68.
[33] P. Duwez, F. Odell, J. Electrochem. Soc. 97 (1950) 299.
[34] S. Tsunekawa, K. Asami, S. Ito, M. Yashima, T. Sugimoto, Appl. Surf. Sci. 252 (2005) 1651.
[35] S.M. Aouadi, P. Filip, M. Debessai, Surf. Coat. Technol. 187 (2004) 177.
[36] P. Prieto, L. Galan, J.M. Sanz, Phys. Rev. B 47 (1993) 1613.
[37] K.L. Haakansson, H.I.P. Johansson, L.I. Johansson, Phys. Rev. B 48 (1993) 2623.
[38] E.M. Moser, B.A. Keller, P. Lienemann, P. Hug, Fresenius', J. Anal. Chem. 346 (1993) 255.
[39] A. Bendavid, P.J. Martin, T.J. Kinder, E.W. Preston, Surf. Coat. Technol. 163–164 (2003) 347.
[40] D. Bekermann, D. Barreca, A. Gasparotto, H.W. Becker, R.A. Fischer, A. Devi, Surf. Coat. Technol. 204 (2009) 404.
[41] M.T. Marques, A.M. Ferraria, J.B. Correia, A.M. Botelho do Rego, R. Vilar, Mater. Chem. Phys. 109 (2008) 174.
[42] G. Jouve, C. Séverac, S. Cantacuzène, Thin Solid Films 287 (1996) 146.
[43] S. Martínez-Méndez, Y. Henríquez, O. Domínguez, L. D'Ornelas, H. Krentzien, J. Mol. Catal. A: Chem. 252 (2006) 226.
[44] Yue Kuo, J. Electrochem. Soc. 139 (1992) 579.
[45] L. Shi, Z. Yang, L. Chen, Y. Qian, Solid State Commun. 133 (2005) 117.
[46] O.Y. Khyzhun, V.A. Kolyagin, J. Alloys Compd. 363 (2004) 32.
[47] E.R. Engbrecht, Y.-M. Sun, S. Smith, K. Pfiefer, J. Bennett, J.M. White, J.G. Ekerdt, Thin Solid Films 418 (2002) 145.
[48] H.B. Michaelson, J. Appl. Phys. 48 (1977) 4729.
[49] W. Schmickler, J.W. Schultze, J.O'M. Bockris, in: B.E. Conway, R.E. White (Eds.), Modern Aspects of Electrochemistry, vol. 17, Plenum, New York, 1986, p. 357.
[50] V.E. Henrich, G. Dresselhaus, H.J. Zeiger, Phys. Rev. Lett. 36 (1976) 1335.
[51] C. Stampfl, A.J. Freeman, Phys. Rev. B 67 (2003) 064108.
[52] H. Imai, M. Matsumoto, T. Miyazaki, S. Fujieda, A. Ishihara, M. Tamura, K. Ota, Appl. Phys. Lett. 96 (2010) 191905.
[53] W. Göpel, J. Vac. Sci. Technol. 15 (1978) 1298.
[54] A.L. Lisebigler, G. Lu, J.T. Yates Jr., Chem. Rev. (Washington, D.C.) 95 (1995) 735.
[55] C. Descorme, Y. Madier, D. Duprez, J. Catal. 196 (2000) 167.
[56] J.M. Blaisdell, A.B. Kunz, Phys. Rev. B 29 (1984) 988.
[57] M. Witko, R. Tokarz-Sobieraj, Catal. Today 91–92 (2004) 171.
[58] E. Miyazaki, I. Yasumori, Surf. Sci. 55 (1976) 747.